Contribution from Rocketdyne, a Division of Rockwell International, Canoga Park, California 91304

Chlorine Trifluoride Dioxide. Vibrational Spectrum, Force Constants, and Thermodynamic Properties

KARL O. CHRISTE* and E. C. CURTIS

Received March 16, 1973

The infrared spectra of gaseous, solid, and matrix-isolated ClF_3O_2 and the Raman spectra of gaseous and liquid ClF_3O_2 are reported. Twelve fundamental vibrations were observed, consistent with a structure of symmetry C_{2v}. A modified valence force field and thermodynamic properties were computed for ClF_3O_2.

Introduction

A brief note on the existence of ClF_3O_2 was recently published by Christe.[1] In a subsequent paper,[2] more details on its synthesis and physical properties were given. Proof for a pseudo-trigonal-bipyramidal structure of symmetry C_{2v} was obtained[2] from its ^{19}F nmr spectrum, which showed an AB_2 pattern with strong evidence for the two equivalent fluorine atoms occupying the apical positions. In this paper, we report the complete vibrational spectrum, force constants, and thermodynamic properties of ClF_3O_2.

Experimental Section

The synthesis and purification of ClF_3O_2 has previously been described.[1,2] The sample used in this investigation showed no detectable impurities except for small amounts of $FClO_2$ which easily forms during handling and cannot be separated from ClF_3O_2 by fractional condensation.[2] The amount of $FClO_2$ formed, however, could be minimized by thorough passivation of the stainless steel–Teflon FEP vacuum system with BrF_5 and ClF_3. For example, the infrared spectrum of gaseous ClF_3O_2 at 700 mm pressure showed the presence of less than 0.1 mol % of $FClO_2$.

The infrared spectra were recorded on a Perkin-Elmer Model 457 spectrophotometer in the range of 4000–250 cm^{-1}. The instrument was calibrated by comparison with standard gas calibration points.[3] The gas cell was made of Teflon and had a path length of 5 cm and AgCl windows. The apparatus, materials, and technique used for the matrix-isolation study have previously been described.[4,5] Raman spectra were recorded on a Cary Model 83 spectrophotometer using the 4880-Å line of an Ar ion laser as the exciting line. A stainless steel cell with Teflon O rings and sapphire windows was used for obtaining the spectrum of the gas. The design of this cell was similar to that of a cell described previously.[6] The spectrum of the liquid was obtained using a Teflon FEP capillary as the sample container in the transverse excitation–transverse viewing mode.

Results and Discussion

Vibrational Spectra. Figure 1 shows the infrared spectra of gaseous, solid, and N_2-matrix-isolated ClF_3O_2 and the Raman spectra of gaseous and liquid ClF_3O_2 at various concentrations. The spectra of solid ClF_3O_2 were corrected for small amounts of $FClO_2$. The $FClO_2$ bands were verified by depositing pure $FClO_2$ on top of the ClF_3O_2 sample and observing the relative growth rates of the bands. Figure 2 shows the most intense infrared bands of gaseous and matrix-isolated ClF_3O_2 at higher resolution allowing some conclusions about the band contours and the determination of the ^{35}Cl–^{37}Cl isotopic shifts. Table I lists the observed frequencies. Table II lists the fundamental vibrations of ClF_3O_2 and their assignment compared to those of the related species ClF_3,[7] ClF_3O,[8] $ClF_2O_2^-$,[9] ClF_4^+,[10] and ClO_2^+.[11]

The structure of ClF_3O_2 can be derived from a trigonal bipyramid, in which the two oxygen ligands could occupy both apical (I), one apical and one equatorial (II), or two equatorial (III) positions. (See Chart I.) These three models be-

Chart I

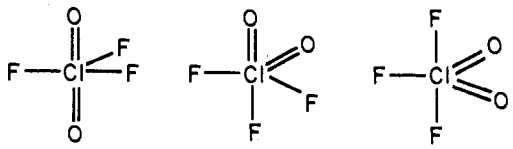

I II III

	I	II	III
Point group	D_{3h}	C_s	C_{2v}
Total no. of fundamentals	8	12	12
Infrared active	5	12	11
Raman active	6	12	12
Polarized Raman bands	2	8	5

long to different point groups and should differ markedly in their vibrational spectra. The observation of a total of 12 fundamentals for ClF_3O_2 (see Figures 1 and 2 and Table I) with a minimum of ten bands being active in the infrared and the Raman spectra, together with the occurrence of four or five polarized Raman bands, rule out point group D_{3h} and favor C_{2v} over C_s. Additional strong evidence for symmetry C_{2v} consists of the relative infrared and Raman intensities and of the frequency separation of the ClF_2 stretching modes, indicating a highly symmetric, *i.e.*, approximately linear, FClF arrangement. Comparison with the vibrational spectra of a number of related species having geometries similar to that of model III (see Table II) also supports model III. This conclusion in favor of model III, reached exclusively on the basis of the observed vibrational spectrum, is in excellent agreement with the observed ^{19}F nmr spectrum[2] and the general observation[12] that, in trigonal-bipyramidal molecules, the most electronegative ligands always occupy the apical positions.

The 12 fundamentals expected for an XY_3Z_2 molecule of symmetry C_{2v} are classified as $5\ A_1 + A_2 + 3\ B_1 + 3\ B_2$. All of these should be active in both the infrared and Raman spectra except for the A_2 mode which should be only Raman

(1) K. O. Christe, *Inorg. Nucl. Chem. Lett.*, **8**, 457 (1972).
(2) K. O. Christe and R. D. Wilson, *Inorg. Chem.*, **12**, 1356 (1973).
(3) E. K. Plyler, A. Danti, L. R. Blaine, and E. D. Tidwell, *J. Res. Nat. Bur. Stand.*, 64, 841 (1960).
(4) K. O. Christe and D. Pilipovich, *J. Amer. Chem. Soc.*, 93, 51 (1971).
(5) K. O. Christe, *Spectrochim. Acta, Part A*, 27, 631 (1971).
(6) E. L. Gasner and H. H. Claassen, *Inorg. Chem.*, **6**, 1937 (1967).
(7) H. Selig, H. H. Claassen, and J. H. Holloway, *J. Chem. Phys.*, **52**, 3517 (1970).
(8) K. O. Christe and E. C. Curtis, *Inorg. Chem.*, **11**, 2196 (1972).
(9) K. O. Christe and E. C. Curtis, *Inorg. Chem.*, **11**, 35 (1972).
(10) K. O. Christe and W. Sawodny, to be submitted for publication.
(11) K. O. Christe, C. J. Schack, D. Pilipovich, and W. Sawodny, *Inorg. Chem.*, **8**, 2489 (1969).
(12) R. F. Hudson, *Angew. Chem., Int. Ed. Engl.*, **6**, 749 (1967).

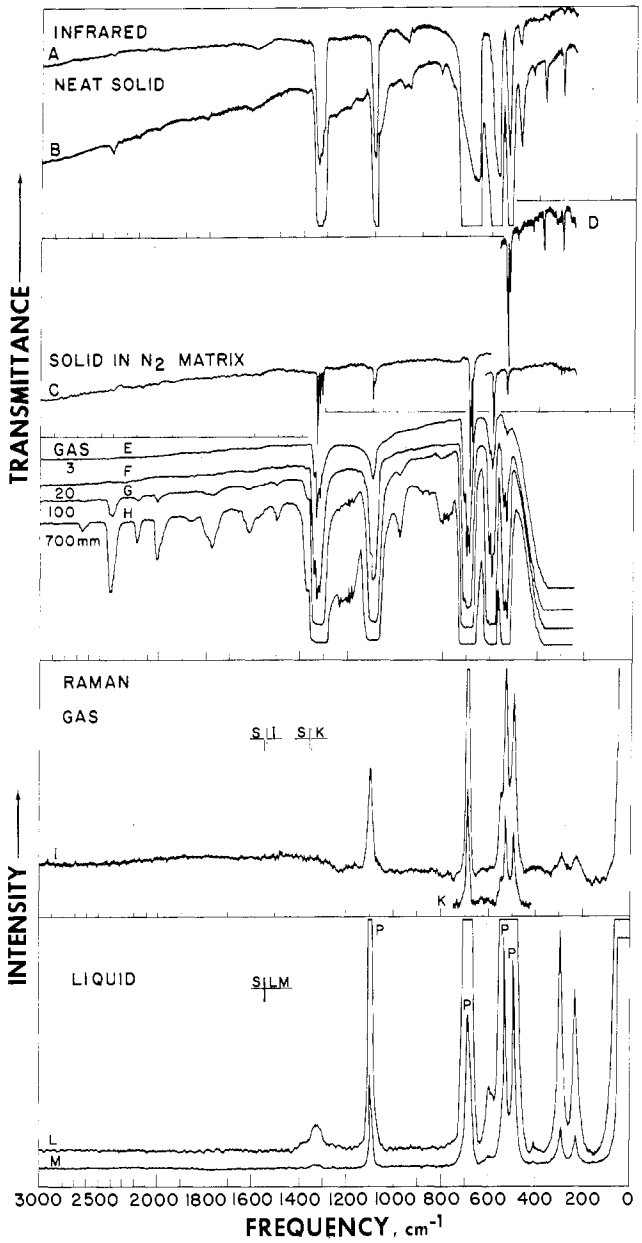

Figure 1. Infrared and Raman spectra of ClF_3O_2. Traces A and B represent the infrared spectra of 22.3 and 230 μmol, respectively, of neat solid ClF_3O_2 at 4°K; traces C and D, the infrared spectra of 0.89 and 20.6 μmol, respectively, of ClF_3O_2 in a N_2 matrix (mole ratio 1:760) at 4°K; traces E–H, the infrared spectra of gaseous ClF_3O_2 at the denoted pressures in a 5-cm path length cell; traces I and K, the Raman spectra of gaseous ClF_3O_2 at 4 atm pressure in a stainless steel cell with sapphire windows; traces L and M, the Raman spectra at two different recorder voltages, respectively, of liquid ClF_3O_2 in a Teflon FEP capillary at 25°; S indicates spectral slit widths and P indicates polarized bands.

active. The strong bands at about 1327 and 1093 cm^{-1} have frequencies too high for any Cl–F stretching modes and, hence, must be assigned to the antisymmetric and symmetric ClO_2 stretching modes, respectively. The antisymmetric axial F–Cl–F stretching mode should occur in the 600–800-cm^{-1} frequency range, be of very high infrared and very low Raman intensity, and by comparison with ClF_3O[8] and ClF_3[7] show a ^{35}Cl–^{37}Cl isotopic shift of about 11 cm^{-1}. Consequently, this mode must be assigned to the bands observed at 686.3 and 674.7 cm^{-1} in the N_2 matrix. The symmetric axial F–Cl–F stretching mode should occur in the 450–570-cm^{-1} frequency range and be of high intensity in the Raman

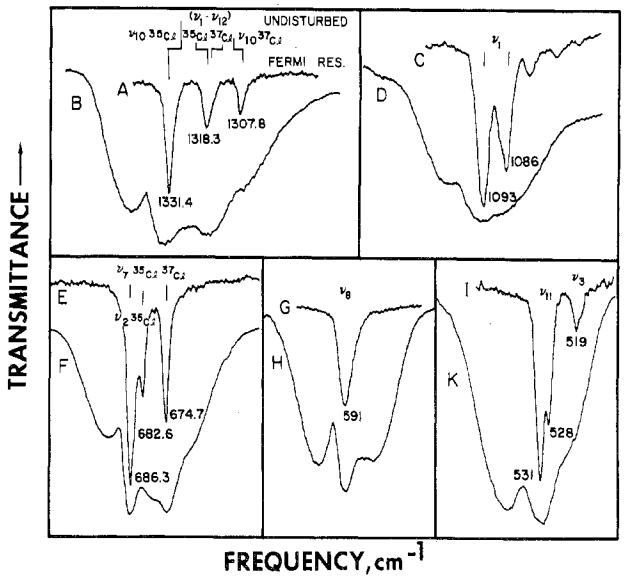

Figure 2. Principal infrared bands of gaseous and N_2-matrix-isolated ClF_3O_2 recorded at tenfold scale expansion under higher resolution conditions. The frequency denotations refer to the matrix-isolation spectra. The frequency scale of the gas bands has been slightly shifted to line up the matrix band centers with the corresponding Q branches of the gas band contours.

and of very low intensity in the infrared spectrum. There are two intense polarized Raman bands at 520 and 487 cm^{-1}, respectively, which might be assigned to this mode. Since the 487-cm^{-1} band is of much lower infrared intensity (for an ideal linear, symmetric F–Cl–F group, this mode should be infrared inactive and indeed was not observed for gaseous ClF_3O_2), it is assigned to the symmetric axial FClF stretching mode. The fifth stretching mode involving the equatorial fluorine is expected to occur between 650 and 800 cm^{-1}, to be of medium to strong infrared intensity, and to give rise to an intense polarized Raman line. Clearly, this mode must be assigned to the 682.6-cm^{-1} band in the matrix and the 683-cm^{-1} Raman band. Comparison with ClF_3O[8] and ClF_3[7] indicates a ^{35}Cl–^{37}Cl isotopic shift of about 7 cm^{-1} for this mode. Its ^{37}Cl part could not directly be observed for the matrix-isolated sample owing to its accidental coincidence with the much more intense ^{37}Cl antisymmetric FClF stretching mode.

The remaining seven bands must be assigned to the deformation modes. Of these, only the A_2 torsion mode ideally should be infrared inactive. Since the Raman band at about 410 cm^{-1} shows no counterpart in the infrared spectrum of the gas, it is assigned to this torsion mode. The 520-cm^{-1} Raman band is clearly polarized and, hence, must belong to species A_1. Based on its relatively high frequency, it must represent the ClO_2 scissoring mode and not the axial F–Cl–F deformation. Based on the observed Fermi resonance (see below) between the 1327-cm^{-1} band and the 1093 + 222 cm^{-1} combination band, the 222- and 1327-cm^{-1} bands must belong to the same symmetry species. Consequently, the 222-cm^{-1} band must represent the B_2 axial F–Cl–F deformation. There are four bands occurring at about 590, 530, 370, and 290 cm^{-1}, respectively, left for assignment. Two of these represent a rocking and wagging motion, respectively, of the ClO_2 group and, therefore, should have higher frequencies than the two remaining FClF deformations. Assignment of the 591-cm^{-1} band to the ClO_2 wag and of the 531-cm^{-1} band to the ClO_2 rock can be made based on the observed gas-phase band contours and the observed ^{35}Cl–^{37}Cl isotopic splittings (see Figure 2, traces G–K). The 591-cm^{-1}

Table I. Vibrational Spectra of ClF_3O_2 and Their Assignment in Point Group C_{2v}

Obsd freq, cm^{-1}, and intens[a]						
Infrared			Raman			
Solid						
Gas	Matrix isolated	Neat	Gas	Liquid	Assignment	
2655 vw					$2 \times 1327 = 2654$	$2\nu_{10}$ (A_1)
2415 vw	2420, 2405, 2385 vs	2405 vw			$1093 + 1327 = 2420$	$\nu_1 + \nu_{10}$ (B_2)
2184 vw		2180 vw			$2 \times 1093 = 2186$	$2\nu_1$ (A_1)
2012 vw	2012 vw	2010 vw			$683 + 1327 = 2010$	$\nu_2 + \nu_{10}$ (B_2)
1860 vw		1850 vw			$520 + 1327 = 1847$	$\nu_3 + \nu_{10}$ (B_2)
1776 vw					$1093 + 695 = 1788$	$\nu_1 + \nu_7$ (B_1)
					$1093 + 683 = 1776$	$\nu_1 + \nu_2$ (A_1)
1625 vw					$1093 + 531 = 1624$	$\nu_1 + \nu_{11}$ (B_2)
1615 vw		1610 vw			$1093 + 520 = 1613$	$\nu_1 + \nu_3$ (A_1)
					$286 + 1327 = 1613$	$\nu_5 + \nu_{10}$ (B_2)
1579 vw					$1093 + 487 = 1580$	$\nu_1 + \nu_4$ (A_1)
1499 vw		1495 vw			$2 \times 487 + 520 = 1494$	$2\nu_4 + \nu_3$ (A_1)
					$683 + 286 + 531 = 1500$	$\nu_2 + \nu_5 + \nu_{11}$ (B_2)
1375 vw		1375 vw			$683 + 695 = 1378$	$\nu_2 + \nu_7$ (B_1)
1366 vw	1365 vw				$2 \times 683 = 1366$	$2\nu_2$ (A_1)
1341, 1331 vs	1331.4 s	1327 s		1320 (0.1) br		$\nu_{10}(^{35}Cl)$ (B_2)
1317	1318.8 ms	1315 m, sh			$1093 + 222 = 1315$	$\nu_1 + \nu_{12}$ (B_2)
1306	1307.8 ms	1305 m, sh				$\nu_{10}(^{37}Cl)$ (B_2)
1230 vs	1230 vw				$520 + 695 = 1215$	$\nu_3 + \nu_7$ (B_1)
1218 vw	1218 vw				$683 + 531 = 1214$	$\nu_2 + \nu_{11}$ (B_2)
	1207 vw	1200 vw			$683 + 520 = 1203$	$\nu_2 + \nu_3$ (A_1)
1195 vw	1203 vw				$2 \times 592 = 1184$	$2\nu_8$ (A_1)
1186 vw		1150 vw			$487 + 695 = 1182$	$\nu_4 + \nu_7$ (B_1)
1174 vw	1173, 1169 vw				$683 + 487 = 1170$	$\nu_2 + \nu_4$ (A_1)
	1116 vw				$417 + 695 = 1112$	$\nu_6 + \nu_7$ (B_2)
					$520 + 592 = 1112$	$\nu_3 + \nu_8$ (B_1)
1093 s	1093 ms					$\nu_1(^{35}Cl)$ (A_1)
			1093 (3.5)	1090 (4.1) pol[b]		
	1086 m					$\nu_1(^{37}Cl)$ (A_1)
	1080 vw, 1073 vw, 1065 vw	1070 vw, sh			$695 + 372 = 1067$, $2 \times 531 = 1062$	$\nu_7 + \nu_9$ (A_1), $2\nu_{11}$ (A_1)
985 vw					$286 + 695 = 981$	$\nu_5 + \nu_7$ (B_1)
978 vw	974 vw	968 vw			$2 \times 487 = 974$	$2\nu_4$ (A_1)
881 vw					$286 + 592 = 878$	$\nu_5 + \nu_8$ (B_1)
856 vw					$487 + 372 = 859$	$\nu_4 + \nu_9$ (B_1)
805, 797 vw	810 vw	806 vw			$520 + 286 = 806$	$\nu_3 + \nu_5$ (A_1)
786 vw					$417 + 372 = 789$	$\nu_6 + \nu_9$ (B_2)
772 vw		760 sh, vw			$487 + 286 = 773$	$\nu_4 + \nu_5$ (A_1)
758 vw					$531 + 222 = 753$	$\nu_{11} + \nu_{12}$ (A_1)
702, 695, 687 sh, 683, 679 sh vs	686.3 vs, 682.6 m, 674.7 s	655 vs, br, 700 sh, s	683 (10)	675 (6.5) pol		$\nu_7(^{35}Cl)$ (B_1), $\nu_2(^{35}Cl)$ (A_1), $\nu_7(^{37}Cl)$ (B_1)
593 s	591 ms	570 s		586 (0.1)		ν_8 (B_1)
543, 531 m	531 m, 528 mw	527 m	540 sh	530 sh		$\nu_{11}(^{35}Cl)$ (B_2), $\nu_{11}(^{37}Cl)$ (B_2)
520 sh, mw	519 w	520 sh, w	520 (7.5)	518 (10) pol		ν_3 (A_1)
	487 vw	473 mw	487 (6.1)	481 (9.0) pol		ν_4 (A_1)
	417 vw	417 vw		402 (0+)		ν_6 (A_2)
	372 w	368 w				ν_9 (B_1)
	287 w	290 w	285 (0.9)	285 (1.6)		ν_5 (A_1)
			222 (0.7)	222 (1.2)		ν_{12} (B_2)

[a] Uncorrected Raman intensities representing the relative peak height; the relative peak widths and, hence, the relative peak heights change from gaseous to liquid ClF_3O_2. [b] Only qualitative polarization measurements could be obtained, owing to the optical activity of the sapphire windows of the gas cell and owing to the tendency of ClF_3O_2 to act as a plasticizer for the Teflon FEP capillaries.

Table II. Vibrational Spectra of ClF_3O_2 Compared to Those of Similar Molecules and Ions

Obsd freq, cm^{-1}, and intens													
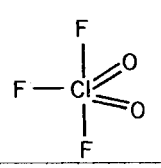		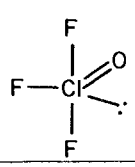 *d*		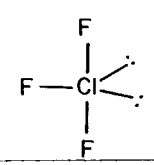 *f*		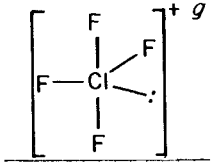 *g*		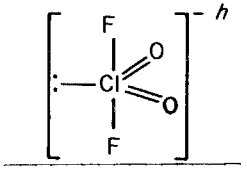 *h*		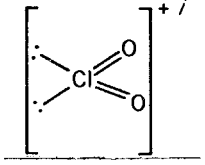 *i*		Assignment for ClF_3O_2 in point group C_{2v}	Approx description of mode[j]
Ir	R	Ir	R	Ir	R	Ir	R	Ir	R	Ir	R		
1093 s	1093 (4) p	(1222)		...		...		1070 s	1076 (10)	1044 s	1044 (10)	A_1 ν_1	Sym ClO_2 str
683 m	683 (10) p	686 s	694 (2.4) p	752 s	752 s, p	830–810		...				ν_2	ClF_{eq} str
519 w	520 (8) p	...		...		...		559 m	559 (1.2)	521 s	521 (3)	ν_3	ClO_2 scissor
487 vw	487 (6) p	478 mw	482 (10) p	530 m	529 vs, p	568 w	567 (7)	330–370 m	363 (10)		...	ν_4	Sym $F_{ax}ClF_{ax}$ str
287 w	285 (1)	*c, e*	224 (0.4) p	328 s	329 w, p	*c*	237 (1)	*c*	198 (0.7)		...	ν_5	$F_{ax}ClF_{ax}$ scissor in ClF_3 plane
(417)[a]	402 (0+)	412 w	414 (0.2) dp		...		474 (1)		480 (1)		...	A_2 ν_6	Torsion
695 vs		652 vs		702 vs		770 vs		510 vs			...	B_1 ν_7	Antisym $F_{ax}ClF_{ax}$ str
592 s	586 (0+)				...			330–370 m	337 (8)		...	ν_8	ClO_2 wag
		499 m	500 (1)			536 mw	538 (2)						
372 w				442 w	431 w, dp			...			...	ν_9	Antisym $F_{eq}ClF_{2ax}$ def in ClF_3 plane
1327[b] vs	1320 (0+)	(1222)		...		...		1225 vs	1221 (0.8)	1296 vs	1296 (1)	B_2 ν_{10}	Antisym ClO_2 str
531 m	530 (1)			...		...					...	ν_{11}	ClO_2 rock
		323 mw[e]	319 (0.1)					330–370 m	378 (8)				
c	222 (1)			328 s	329 w	386 m	388 (0+)				...	ν_{12}	$F_{ax}ClF_{ax}$ scissor out of ClF_3 plane

[a] Observed only for solid ClF_3O_2. [b] Frequency corrected for disturbance by Fermi resonance. [c] Below frequency range of spectrometer used. [d] K. O. Christe and E. C. Curtis, *Inorg. Chem.*, **11**, 2196 (1972). [e] According to the potential energy distribution, the 224- and 320-cm^{-1} modes are an almost equal mixture of the corresponding symmetry coordinates and, hence, not very characteristic. [f] H. Selig, H. H. Claassen, and J. H. Holloway, *J. Chem. Phys.*, **52**, 3517 (1970). [g] K. O. Christe and W. Sawodny, to be submitted for publication. [h] K. O. Christe and E. C. Curtis, *Inorg. Chem.*, **11**, 35 (1972). [i] K. O. Christe, C. J. Schack, D. Pilipovich, and W. Sawodny, *ibid.*, 8, 2489 (1969). [j] The modes in the B_1 block are highly mixed (see PED, Table VII) and, therefore, difficult to associate with the frequencies.

Table III. Symmetry Coordinates[a] for ClF_3O_2

A_1	S_1	$(1/\sqrt{2})(\Delta D_1 + \Delta D_2)$
	S_2	ΔR
	S_3	$(1/\sqrt{6})(2\Delta\alpha - \Delta\gamma_1 - \Delta\gamma_2)$
	S_4	$(1/\sqrt{2})(\Delta r_1 + \Delta r_2)$
	S_5	$(1/\sqrt{12})(2\Delta\beta_1 + 2\Delta\beta_2 - \Delta\delta_1 - \Delta\delta_2 - \Delta\delta_3 - \Delta\delta_4)$
	S_{r1}	$(1/\sqrt{3})(\Delta\alpha + \Delta\gamma_1 + \Delta\gamma_2) = 0$
	S_{r2}	$(1/\sqrt{6})(\Delta\beta_1 + \Delta\beta_2 + \Delta\delta_1 + \Delta\delta_2 + \Delta\delta_3 + \Delta\delta_4) = 0$
A_2	S_6	$(1/\sqrt{4})(\Delta\delta_1 - \Delta\delta_2 - \Delta\delta_3 + \Delta\delta_4)$
B_1	S_7	$(1/\sqrt{2})(\Delta r_1 - \Delta r_2)$
	S_8	$(1/\sqrt{4})(\Delta\delta_1 - \Delta\delta_2 + \Delta\delta_3 - \Delta\delta_4)$
	S_9	$(1/\sqrt{2})(\Delta\beta_1 - \Delta\beta_2)$
B_2	S_{10}	$(1/\sqrt{2})(\Delta D_1 - \Delta D_2)$
	S_{11}	$(1/\sqrt{2})(\Delta\gamma_1 - \Delta\gamma_2)$
	S_{12}	$(1/\sqrt{4})(\Delta\delta_1 + \Delta\delta_2 - \Delta\delta_3 - \Delta\delta_4)$

[a] S_{r1} and S_{r2} are the redundant coordinates and $\delta_1 = \angle O_1ClF_2$, $\delta_2 = \angle O_1ClF_3$, $\delta_3 = \angle O_2ClF_2$, and $\delta_4 = \angle O_2ClF_3$.

band shows a Q-R branch splitting for $^{35}ClF_3O_2$ of about 8 cm^{-1} comparable to that observed for the antisymmetric FClF stretch, ν_7 (B_1). The 531-cm^{-1} band exhibits a missing Q branch and a P-R branch separation of about 11 cm^{-1} comparable to that observed for the antisymmetric ClO_2 stretch, ν_{10} (B_2). Furthermore, the 531-cm^{-1} band shows a larger ^{35}Cl-^{37}Cl isotopic splitting than the one at 591 cm^{-1} in agreement with the values (see Table IV) computed for the ClO_2 rocking and wagging motions, respectively. The remaining two bands at 286 and 372 cm^{-1} are assigned to the axial F-Cl-F scissoring mode ν_5 (A_1) and the antisymmetric in-plane ClF_3 deformation mode, ν_9 (B_1), respectively. This assignment is based on the observed frequencies and the relative infrared and Raman intensities. The assignment of the 286-cm^{-1} Raman band to an A_1 mode is further supported by the fact that it appears to be weakly polarized. The excellent fit between all the observed and computed combination bands and overtones (see Table I) without violation of the selection rules ($B_1 + B_2 = A_2$ and $A_1 + A_2 = A_2$ combinations are infrared forbidden) also suggests the correctness of the above assignments.

The observation of three relatively intense bands in the N_2 matrix for the antisymmetric ClO_2 stretching mode, ν_{10} (B_2), requires further explanation. For this mode, a ^{35}Cl-^{37}Cl isotopic splitting of about 15 cm^{-1} might be predicted by comparison with that observed for related ClO_2^+.[11] The combination band 1093 + 222 = 1315 cm^{-1} should show a considerably smaller ^{35}Cl-^{37}Cl isotopic splitting of about 8 cm^{-1} (see Table IV) and based on its frequency fall between the ^{35}Cl and ^{37}Cl isotopic bands of ν_{10}. As shown schematically in Figure 2, Fermi resonance between ν_{10} and $\nu_1 + \nu_{12}$ will increase the frequency separation between the ^{35}Cl and ^{37}Cl components of ν_{10} and decrease that between the two isotopic combination bands. This assignment is supported by the observed bandwidths at half-height which are similar (~2.0 cm^{-1}) for the 1331.4- and 1307.8-cm^{-1} bands but larger (~3.0 cm^{-1}) for the 1318.8-cm^{-1} band. The disturbance by Fermi resonance can also account for the strongly increased intensity of the combination band. The fact that the frequency of the 1318.3-cm^{-1} band is closer to 1307.8 cm^{-1} than to 1331.4 cm^{-1} agrees with the observed relative intensities. The 1307.8-cm^{-1} band has lost relatively more of its original intensity as demonstrated by the observed intensity ratio of 1:4.4 for the 1307.8- and 1331.4-cm^{-1} bands. For undisturbed ^{35}Cl-^{37}Cl isotopic species, this ratio should be 1:3.07.

The observed gas-phase infrared band contours are complicated by the ^{35}Cl-^{37}Cl isotopic splittings, Fermi resonance, and two double coincidences of ν_7 with ν_2 and of ν_{11} with ν_3, respectively. However, for most of the bands, the R branches of the ^{35}Cl isotope are well separated (see Figure 2). Since the geometry of ClF_3O_2 of symmetry C_{2v} can be estimated (see below), the three principal moments of inertia were computed resulting in $A = 0.150$, $B = 0.106$, and $C = 0.095$ cm^{-1}. Based on these values, the infrared band contours were estimated for ClF_3O_2, according to the method of Ueda and Shimanouchi.[13] Using No. 33 of Ueda's Figure 3,[13] one should expect for the B_1 modes an A-type band contour with a sharp Q branch and a P-R branch separation of about 16 cm^{-1}. As can be seen from Figure 2, the 686- and 591-cm^{-1} bands show the predicted band shape and branch separation and, therefore, may be assigned with confidence to ν_7 and ν_8, respectively. The 1331- and 531-cm^{-1} bands do not show a Q branch as expected for B-type bands of species B_2. Consequently, the observed band contours are consistent with the proposed structure of symmetry C_{2v} and the assignments listed in Table I.

Comparison between the vibrational spectrum of ClF_3O_2 and those of related species (Table II) shows good agreement and strongly supports the above assignments for ClF_3O_2. Two features in the ClF_3O_2 spectrum, however, require further comment. The ClO_2 scissoring mode, ν_3 (A_1), is unexpectedly intense in the Raman spectrum. Since the frequency of ν_3 is close to that of the intense ν_2 (A_1) mode and since these motions could easily couple (as indicated by the normal-coordinate transformation L^{-1} and to some extent by the PED), this represents a plausible explanation for its high intensity. Alternate explanations such as Fermi resonance between the symmetric axial FClF stretching mode ν_4 and 222 + 286 = 508 cm^{-1} can be ruled out because they belong to different symmetry species. Resonance between ν_3 and ν_4 can also be eliminated because the observed combination bands involving either ν_3 or ν_4 show a good frequency fit, indicating that the fundamentals are undisturbed. Second, the frequencies of the two axial FClF scissoring modes (in and out of the ClF_3 plane, respectively) are strongly influenced by the point group of the corresponding molecules and by the presence or absence of other modes in the same symmetry species and, hence, are difficult to correlate. Furthermore, in ClF_3O, these two frequencies are not characteristic and are an almost equal mixture of the corresponding symmetry coordinates.[8]

Force Constants. The potential and kinetic energy metrics for ClF_3O_2 were computed by a machine method.[14] The geometry assumed for this computation was $D(ClO) = 1.40$ Å, $R(ClF_{eq}) = 1.62$ Å, $r(ClF_{ax}) = 1.72$ Å, $\alpha(OClO) = 130°$, $\beta(F_{eq}ClF_{ax}) = \delta(OClF_{ax}) = 90°$, and $\gamma(OClF_{eq}) = 115°$, based on the observed geometries of ClF_3[15] and $FClO_3$[16] and a correlation[17] between ClO bond length and stretching frequency. The deviation of the OClO bond angle from the ideal 120° was estimated by comparison with the known geometries of SF_4O[18] and $FClO_3$.[16]

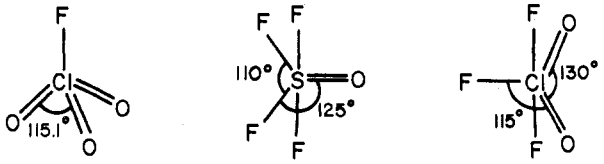

The symmetry coordinates used for ClF_3O_2 are given in Table III. The bending coordinates were weighted by unit (1 Å) distance so the stretching force constants have units of mdyn/Å, the deformation force constants units of mdyn Å/radian^2, and the stretch-bend interaction constants have units of mdyn/radian. The G matrix and Z transformation were found numerically by the computer and, hence, are not given here.

The force constants were adjusted by trial and error with the aid of a computer to give an exact fit between the observed and computed frequencies. Owing to the underdetermined nature (28 symmetry force constants and 12 frequencies) of the problem, a diagonal force field was com-

(13) T. Ueda and T. Shimanouchi, *J. Mol. Spectrosc.*, **28**, 350 (1968).

(14) E. C. Curtis, *Spectrochim. Acta, Part A*, **27**, 1989 (1971).
(15) D. F. Smith, *J. Chem. Phys.*, **21**, 609 (1953).
(16) A. H. Clark, B. Beagley, and D. W. J. Cruickshank, *Chem. Commun.*, 14 (1968).
(17) E. A. Robinson, *Can. J. Chem.*, 41, 3021 (1963).
(18) J. L. Hencher, D. W. Cruickshank, and S. H. Bauer, *J. Chem. Phys.*, **48**, 518 (1968).

Table IV. Observed Frequencies (cm^{-1}), Symmetry Force Constants,[a] and Computed and Observed ^{35}Cl and ^{37}Cl Isotopic Shifts (cm^{-1})

		Freq		F	$\Delta\nu$(comp)	$\Delta\nu$(obsd)
A_1	ν_1	1093	$F_{11} = f_D + f_{DD}$	9.14	7.1	7.2
			$F_{13} = (1/\sqrt{3})(2f_{D\alpha} - f_{D\gamma} - f_{D\gamma'})$	0.70		
	ν_2	683	$F_{22} = f_R$	3.35	6.8	~7
			$F_{23} = (\sqrt{2/3})(f_{R\alpha} - f_{R\gamma})$	−0.30		
	ν_3	520	$F_{33} = (1/3)(2f_\alpha + f_\gamma + f_{\gamma\gamma} - 4f_{\alpha\gamma})$	1.27	0.8	~1
	ν_4	487	$F_{44} = f_r + f_{rr}$	2.65	0	
	ν_5	286	$F_{55} = (1/3)(2f_\beta + f_\delta + 2f_{\beta\beta} + f_{\delta\delta} + f_{\delta\delta'} + f_{\delta\delta''} - 4f_{\beta\delta} - 4f_{\beta\delta'})$	1.37	0.5	
A_2	ν_6	417	$F_{66} = f_\delta - f_{\delta\delta} - f_{\delta\delta'} + f_{\delta\delta''}$	1.13	0	
B_1	ν_7	695	$F_{77} = f_r - f_{rr}$	2.75	11.7	11.6
			$F_{78} = \sqrt{2}(f_{r\delta} - f_{r\delta'})$	0.70		
			$F_{79} = f_{r\beta} - f_{r\beta'}$	0.20		
	ν_8	592	$F_{88} = f_\delta - f_{\delta\delta} + f_{\delta\delta'} - f_{\delta\delta''}$	2.15	0	~0
			$F_{89} = \sqrt{2}(f_{\beta\delta} - f_{\beta\delta'})$	−0.44		
	ν_9	372	$F_{99} = f_\beta - f_{\beta\beta}$	1.31	1.0	
B_2	ν_{10}	1327	$F_{10,10} = f_D - f_{DD}$	9.33	16.8	16–17[b]
	ν_{11}	531	$F_{11,11} = f_\gamma - f_{\gamma\gamma}$	1.63	2.2	2.6
	ν_{12}	222	$F_{12,12} = f_\delta + f_{\delta\delta} - f_{\delta\delta'} - f_{\delta\delta''}$	0.78	0.6	

[a] Stretching constants in mdyn/Å, deformation constants in mdyn Å/radian^2, and stretch–bend interaction constants in mdyn/radian; symmetry force constants not shown were assumed to be zero. [b] Corrected for Fermi resonance interaction with $(\nu_1 + \nu_{12})$.

puted assuming all off-diagonal symmetry force constants equal to zero. In the A_1 and B_1 block, however, nonzero values were required for several off-diagonal constants to be able to reproduce the observed frequencies. The quality of the resulting force field was examined by comparing the computed ^{35}Cl–^{37}Cl isotopic shifts with those observed. The observed Cl isotopic shifts were then used to improve the force field by introducing off-diagonal constants until the calculated isotopic shifts agreed with the observed ones. Those interaction constants not significantly influencing the isotopic shift were not changed while those introduced were required to achieve a fit between observed and computed isotopic shifts. The force field is still not unique and other solutions are certainly possible. Species A_1 contains 15 symmetry force constants. Of these, three off-diagonal terms, *i.e.*, F_{14}, F_{24}, and F_{34}, may be neglected[19] since their corresponding G matrix elements are zero. Therefore, eight frequencies (5 ^{35}Cl + 3 ^{37}Cl) are available for obtaining 12 symmetry force constants. In species B_1 and B_2 five frequency values are available for obtaining six symmetry force constants. Numerical experiments indicated that plausible force fields and PED values could be achieved only with values reasonably close to those shown in Table IV. The requirement of a large off-diagonal constant for B_1 has previously also been found for the structurally related pseudo-trigonal-bipyramidal SF_4O molecule.[20]

The internal coordinate stretching force constants can be computed; however, the bending valence force constants cannot be completely separated from the interaction constants without making additional simplifying assumptions (see Table V). The constants of greatest interest are the stretching force constants since they are a measure of the strength of the various bonds. Uncertainty estimates are difficult to make owing to the underdetermined nature of the force field. The value of the Cl=O stretching force constant should have the smallest uncertainty (0.1 mdyn/Å or less) owing to the highly characteristic nature of the ClO_2 stretching modes and the use of isotopic shifts for its computation. Its value of 9.23 mdyn/Å is in excellent agreement with that of 9.37 mdyn/Å found for ClF_3O[8] and the general valence force field values of 9.07 and 8.96 mdyn/Å reported for $FClO_2$[21] and ClO_2^+,[11] respectively. The values

Table V. Internal Force Constants of ClF_3O_2[a,b]

$f_D = 9.23$	$f_{\beta\beta} = 0.09$
$f_R = 3.35$	$f_{r\beta} = -f_{r\beta'} = 0.10$
$f_r = 2.70$	$f_{r\delta} = -f_{r\delta'} = 0.25$
$f_\alpha = 1.41$	$f_{D\alpha} = 0.61$
$f_\beta = 1.40$	$f_{\beta\delta} = -f_{\beta\delta'} = -0.16$
$f_\gamma = 1.33$	$f_{\delta\delta} = -f_{\delta\delta'} = -0.34$
$f_\delta = 1.30$	$f_{\delta\delta''} = -0.17$
$f_{DD} = -0.09$	$f_{\gamma\gamma} = -0.30$
$f_{rr} = -0.04$	$f_{R\alpha} = -0.37$

[a] Stretching constants in mdyn/Å, deformation constants in mdyn Å/radian^2, and stretch–bend interaction constants in mdyn/radian. [b] Only the values of the stretching force constants can be uniquely determined from the symmetry force constants; for the computation of the remaining constants, the following assumptions were made: $f_{r\beta} = -f_{r\beta'}$, $f_{r\delta} = -f_{r\delta'}$, $f_{\beta\delta} = -f_{\beta\delta'}$, $f_{\delta\delta} = -f_{\delta\delta'}$, and $f_{R\gamma} = f_{D\gamma} = f_{\alpha\gamma} = 0$; $f_{\delta\delta}$, $f_{\delta\delta'}$, and $f_{\delta\delta''}$ are the interactions between angles having a common oxygen, fluorine, and no common atom, respectively.

Table VI. ClF Stretching Force Constants (mdyn/Å) of ClF_3O_2 Compared to Those of Pseudo-Trigonal-Bipyramidal ClF_3O,[8] ClF_3,[22] ClF_2^-,[23] and $ClF_2O_2^-$[9]

	f_R	f_r	f_{rr}	$(f_R - f_r)/f_R$
ClF_3	4.2	2.7	0.36	0.36
ClF_3O	3.2	2.3	0.26	0.26
ClF_3O_2	3.4	2.7	−0.04	0.19
ClF_2^-		2.4	0.17	
$ClF_2O_2^-$		1.6	−0.1	

of the ClF stretching force constants are comparable to those previously reported for the related pseudo-trigonal-bipyramidal molecules ClF_3[22] and ClF_3O[8] (see Table VI). In all three molecules, the stretching force constant of the equatorial ClF bond is significantly higher than that of the two axial bonds, although their relative difference decreases with increasing oxidation state of the central atom. The difference in bond strength between equatorial and axial bonds implies significant contributions from semiionic three-center four-electron bonds to the axial ClF bonds. This bonding scheme has previously been discussed in detail[23] for the related pseudo-trigonal-bipyramidal ClF_2^- anion and, hence, will not be repeated.

Inspection of Table VI also reveals that the value of f_r does not depend exclusively on the oxidation state of the central

(19) W. Sawodny, *J. Mol. Spectrosc.*, **30**, 56 (1969).
(20) K. Sathianandan, K. Ramaswamy, S. Sundaram, and F. F. Cleveland, *J. Mol. Spectrosc.*, **13**, 214 (1964).
(21) D. F. Smith, G. M. Begun, and W. H. Fletcher, *Spectrochim. Acta*, **20**, 1763 (1964).
(22) R. A. Frey, R. L. Redington, and A. L. K. Aljibury, *J. Chem. Phys.*, **54**, 344 (1971).
(23) K. O. Christe, W. Sawodny, and J. P. Guertin, *Inorg. Chem.*, **6**, 1159 (1967).

atom. Obviously, formal negative charges (as in the anions) and increasing oxygen substitution facilitate[9] the formation of semiionic bonds and, hence, counteract the influence of the oxidation state of the central atom. It is interesting to note that the relative contribution from semiionic bonding to the axial ClF bonds $[=(f_R - f_r)/f_R]$ decreases from ClF_3 to ClF_3O and ClF_3O_2 (see Table VI). This can be attributed to the decreasing electron density around the central atom with increasing oxidation state, thus making it more difficult to release electron density to the axial fluorine ligands as required for the formation of semiionic bonds.

In summary, the bonding in ClF_3O_2 might be described by the following approximation.[24] The bonding of the three equatorial ligands, ignoring the second bond of the Cl=O double bond, is mainly due to an sp^2 hybrid, whereas the bonding of the two axial ClF bonds involves one delocalized p-electron pair of the chlorine atom for the formation of a semiionic three-center four-electron $p\sigma$ bond.

The potential energy distribution[25] for ClF_3O_2 was obtained from the internal force constants of Table V using a least-squares force field computation code without using least-squares refinement. With this code, we also verified that no computational errors had been made in the trial and error force field computation. The computed PED is given in Table VII. The results were normalized, but the sums do not in all cases add up to 1.0 since the less important terms are not listed. As can be seen from Table VII, most vibrations are reasonably characteristic, except for ν_7 and ν_8, which are mixtures of the symmetry coordinates S_7 and S_8.

Association in the Liquid and Pure Solid. The relatively low boiling point (−21.58°)[2] and Trouton constant (22.13)[2] of ClF_3O_2 imply little association in the liquid phase. This prediction is confirmed by the vibrational spectra of the liquid and the neat solid which exhibit only minor frequency shifts when compared to the spectra of the gas and the matrix-isolated solid. This finding is somewhat surprising since both ClF_3[24] and ClF_3O[8] show a pronounced tendency to associate in the liquid and solid state through bridges involving the axial fluorine atoms. For the pure solid, the infrared spectrum indicates the lowering of symmetry C_{2v} due to slight distortion or a lower site symmetry in the crystal because the A_2 torsion mode, ideally forbidden in the infrared spectrum and not observed for the gas, becomes infrared active. Similarly, the symmetric axial FClF stretching mode, ν_4 (A_1), which was not observed in the infrared spectrum of gaseous ClF_3O_2, gained for solid ClF_3O_2 in relative intensity and was observed as a medium weak band.

Thermodynamic Properties. The thermodynamic properties were computed with the molecular geometry and vibrational frequencies given above assuming an ideal gas at 1 atm pressure and using the harmonic-oscillator rigid-rotor approximation.[26] These properties are given for the range 0–2000°K in Table VIII.

Table VII. Potential Energy Distribution for ClF_3O_2

	Assignment	Freq, cm^{-1}	PED
A_1	ν_1	1093	$0.99f_D + 0.06f_R - 0.06f_{D\alpha}$
	ν_2	683	$0.71f_R + 0.20f_\alpha - 0.13f_{R\alpha} + 0.10f_\gamma + 0.05f_\beta$
	ν_3	520	$0.50f_\alpha + 0.23f_\gamma + 0.22f_R + 0.12f_{R\alpha} - 0.05f_{\gamma\gamma} - 0.05f_{D\alpha}$
	ν_4	487	$1.02f_r$
	ν_5	286	$0.61f_\beta + 0.28f_\delta + 0.14(f_{\beta\delta} - f_{\beta\delta'}) + 0.07(f_{\delta\delta'} - f_{\delta\delta}) + 0.06f_\alpha$
A_2	ν_6	417	$1.15f_\delta + 0.30(f_{\delta\delta} - f_{\delta\delta'}) - 0.15f_{\delta\delta''}$
B_1	ν_7	695	$0.86f_r + 0.39f_\delta - 0.22(f_{r\delta} + f_{r\delta'}) + 0.10(f_{\delta\delta} + f_{\delta\delta'}) + 0.05f_{\delta\delta''}$
	ν_8	592	$0.26f_\delta + 0.25f_r + 0.10(f_{r\delta} + f_{r\delta'}) + 0.07(f_{\delta\delta} + f_{\delta\delta'}) + 0.06f_\beta$
	ν_9	372	$1.10f_\beta - 0.10(f_{\beta\delta} + f_{\beta\delta'}) + 0.08f_\delta - 0.07f_{\beta\beta}$
B_2	ν_{10}	1327	$0.93f_D$
	ν_{11}	531	$0.75f_\gamma + 0.16f_{\gamma\gamma}$
	ν_{12}	222	$1.58f_\delta - 0.41(f_{\delta\delta} + f_{\delta\delta'}) + 0.21f_{\delta\delta''}$

Table VIII. Thermodynamic Properties for ClF_3O_2

T, °K	$C_p°$, cal/mol	$H° - H°_0$, kcal/mol	$-(F° - H°_0)/T$, cal/(mol deg)	$S°$, cal/(mol deg)
0	0	0	0	0
100	10.127	0.847	48.967	57.437
200	16.511	2.179	55.516	66.411
298.15	21.256	4.049	60.375	73.956
300	21.327	4.089	60.459	74.088
400	24.384	6.386	64.711	80.675
500	26.362	8.930	68.484	86.344
600	27.685	11.636	71.881	91.275
700	28.599	14.453	74.968	95.615
800	29.251	17.347	77.795	99.479
900	29.727	20.298	80.400	102.953
1000	30.085	23.289	82.816	106.105
1100	30.360	26.312	85.066	108.985
1200	30.574	29.359	87.171	111.637
1300	30.745	32.425	89.148	114.091
1400	30.883	35.507	91.012	116.375
1500	30.995	38.601	92.775	118.509
1600	31.089	41.705	94.447	120.513
1700	31.167	44.818	96.036	122.400
1800	31.233	47.938	97.551	124.183
1900	31.289	51.064	98.997	125.873
2000	31.337	54.196	100.382	127.480

Acknowledgment. The authors wish to express their gratitude to Mr. R. D. Wilson for his help in the experimental efforts, to Drs. D. Philipovich and C. J. Schack for helpful discussions, and to Dr. D. Lawson of the Jet Propulsion Laboratory for the use of the Raman spectrophotometer. This work was supported by the Office of Naval Research, Power Branch.

Registry No. ClF_3O_2, 38680-84-1.

(24) K. O. Christe, paper presented at the Fourth International Fluorine Symposium, Estes Park, Colo., July 1967.

(25) J. Overend and J. R. Scherer, *J. Chem. Phys.*, **32**, 1289 (1960).

(26) J. E. Mayer and M. G. Mayer, "Statistical Mechanics," Wiley, New York, N. Y., 1940.